Received: 11 January 2017 | Accepted: 24 April 2017

DOI: 10.1111/jace.14947

ORIGINAL ARTICLE

Journal of the American Ceramic Society

Two successive amorphous-to-amorphous phase transformations in TiO_2

Murat Durandurdu

Department of Materials Science and Nanotechnology Engineering, Abdullah Gül University, Kayseri, Turkey

Correspondence
Murat Durandurdu, Department of Materials science and Nanotechnology Engineering, Abdullah Gül University, Kayseri, Turkey.
Email: murat.durandurdu@agu.edu.tr

Funding information
Abdullah Gül University Support Foundation

Abstract

Based on constant pressure ab initio simulations, we propose, for the first time, two successive amorphous-to-amorphous phase transformations for TiO_2. The first one is a gradual phase transformation from a low-density amorphous phase to a high-density amorphous phase, whereas the second one is a first-order phase transformation from the high-density amorphous phase to a very high-density amorphous phase. The low-density amorphous to high-density amorphous phase change is irreversible, whereas the high-density amorphous to very high-density amorphous phase transformation is reversible. The high-density amorphous and very high-density amorphous phases consist of differently coordinated configurations. The sevenfold and ninefold-coordinated arrangements formed in amorphous TiO_2 under pressure are similar to the main building motif of the baddeleyite and cotunnite polymorphs of TiO_2, respectively, while the eightfold-coordinated configuration is different from the local structure of the cubic TiO_2 phase. The electronic structure calculations suggest that both dense amorphous phases present a semiconducting character with a band gap energy less than that of the original low-density amorphous phase.

KEYWORDS
phase transformation, polyamorphism, titanium oxide

1 | INTRODUCTION

Polyamorphism[1] referring to multiple amorphous states with different densities and coordination numbers but the same composition is commonly observed during the high-pressure treatment of tetrahedrally coordinated amorphous systems such as ice[2], silicon[3–6], germanium[7,8], silica[9–12], germinate[13], and chalcogenide glasses.[14–17] Ice shows a first-order phase transformation from a low-density amorphous (LDA) state to a high-density amorphous (HDA) state under pressure.[2] Similar to ice, polyamorphic phase transformation in silicon[3–6] and germanium[7,8] is accompanied by a sharp volume collapse as well and their HDA phase exhibits a metallic character. In a stark contrast to these materials, the amorphous-to-amorphous phase transformation takes place gradually in silica[9–12], germinate[13], and chalcogenide glasses.[14–17] Depending on the temperature and pressure conditions applied, their HDA phase can be quenchable or unquenchable to ambient pressure. In addition to the HDA phase, the presence of a very high-density amorphous (VHDA) phase has been also discussed for some of these materials.[18–20]

Recent investigations have suggested the existence of polyamorphic phase transitions even in more closely structured materials.[21–29] Among these materials, the polyamorphic phase transformation in nanoscale TiO_2 systems has received particular interest[25–31] as they are one of the most promising materials with a wide range of high-tech applications.[28] TiO_2 nanoparticles undergo amorphization with the application of pressure. The resulting state is referred as a HDA phase and locally similar to the sevenfold-coordinated high-pressure monoclinic (baddeleyite) TiO_2

crystal.[25,28,30] Upon pressure release, the HDA-to-LDA phase transformation is observed. Although the local structure of the LDA phase is clearly not known yet, the studies correlate it with the sixfold-coordinated columbite (α-PbO_2)-type crystal.[25,28,30] With the application of pressure, amorphous TiO_2 (a-TiO_2) nanostructures show a reversible LDA-to-HDA phase transformation too.[29] Moreover, depending on the starting structure, the formation of possible different HDA phases is proposed for nanoscale TiO_2 (Ref.29).

Here by basically applying a constant pressure ab initio approach, we compress an a-TiO_2 model up to 75 GPa and find that it undergoes two successive polyamorphic phase transitions. The first one is a LDA-to-HDA phase transformation as reported for nanoscale TiO_2. However, the LDA-HDA phase change in a-TiO_2 is irreversible in a contrast to the phase transformation observed in nanosized TiO_2 systems. The second one is a reversible HDA-to-VDHA phase transformation and is proposed for the first time in this study.

2 | METHOD

All simulations were performed using the SIESTA package.[32] We used the DZP basis (2-2*s*, 6-2*p*, and 5-polarized 2*d* orbitals for O atom and 2-4*s*, 10-3*d*, and 3-polarized 4*p* orbitals for Ti atom), Γ-point for the Brillouin zone sampling, and the NPT ensemble to model a-TiO_2. Pressure and temperature were applied by the Parrinelo-Rahman method[33] and the velocity rescaling approach, correspondingly. We used the generalized gradient approximation of Perdew, Burke, and Ernzerhof[34] to compute the exchange correlation energy and the Troullier-Martins scheme[35] to generate pseudopotentials. To create an a-TiO_2 model, we adopted the anatase phase with 216 atoms (144 O and 72 Ti atoms) as a starting structure and subjected it to 3300 K for 10 ps. Then temperature was reduced to 2200 K in 5.0 ps. At this temperature, the system was thermalized for 20.0 ps and then cooled to 300 K in 30 ps. The time step of each molecular dynamics simulation was chosen to be one femtosecond. Finally, the structure was optimized using the power quenching technique within the NPH ensemble. In order to explore the high-pressure behavior of a-TiO_2, we applied the constant pressure relaxation simulation using the Parrinello-Rahman technique along with the power quenching approach. We increased the external pressure progressively using an increment of 5 GPa. We found that 10 000 time steps were adequate to relax the amorphous structure till the maximum force was at least less than 0.01 eV/Å at each applied pressure. Our prior studies showed that the SIESTA ab initio code successfully reproduced the crystal-to-crystal, amorphous-to-amorphous, and amorphous-to-crystal phase transformations in a wide variety of materials.[36] The ISAACS[37] program was used to obtain some structural information at the atomistic level. The cluster analysis was performed by the Voronoi polyhedra method.[38] A Voronoi polyhedron is denoted by indices $<n_3, n_4, n_5, n_6, \ldots>$, where n_i and $\sum n_i$ give the number of i-edge faces of polyhedron and the total coordination number, respectively.

3 | RESULTS

The variation in volume under the external pressure is provided in Figure 1. The figure clearly shows a smooth volume change up to 20 GPa and then ripples at several pressures, which might be due to the small size of simulation box. At 60 GPa, the volume presents a noticeable discontinuity that perhaps signifies a possible first-order phase transformation in a-TiO_2. The corresponding volume collapse at this pressure is about 5%. Upon decompression from two different pressures, 55 and 75 GPa, the volume shows a hysteresis and the initial volume is never recovered, implying that pressure causes a noticeable densification in a-TiO_2. The densification might be associated with the elimination of the free volume and/or the induction of irreversible higher coordinated arrangements in the amorphous model during the high-pressure treatment.

On the basis of the previous studies on disordered materials, two scenarios can be thinkable for a-TiO_2 under pressure: it can transform to either a crystalline phase or a HDA phase. In order to see which transformation appears in a-TiO_2, we plot the total pair correlation function at

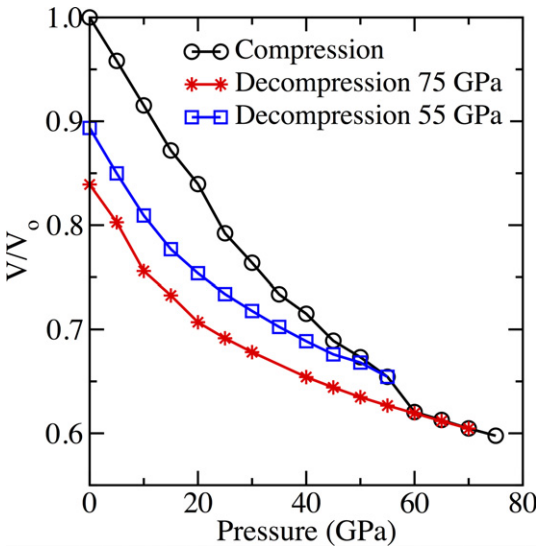

FIGURE 1 The pressure-volume relation of a-TiO_2 on compression and decompression from 55 and 75 GPa [Color figure can be viewed at wileyonlinelibrary.com]

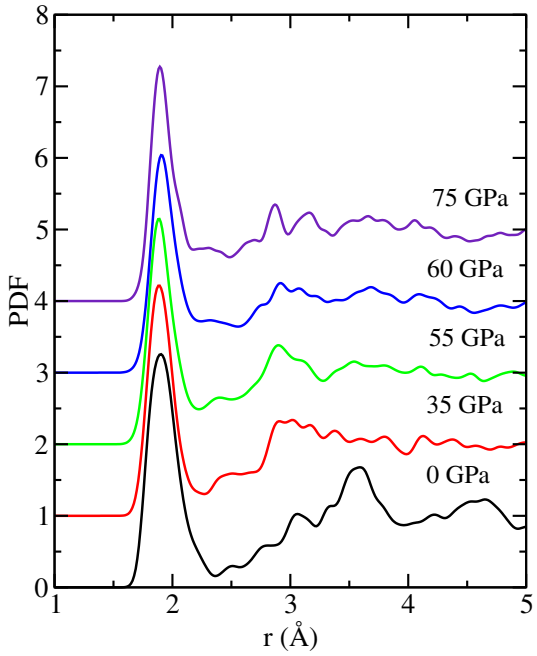

FIGURE 2 The total pair distribution function at selected pressures [Color figure can be viewed at wileyonlinelibrary.com]

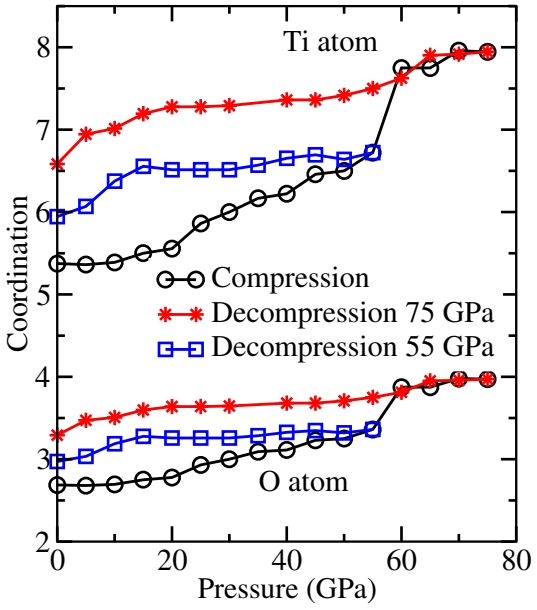

FIGURE 3 The modification in average Ti and O coordination numbers as a function of pressure on compression and decompression [Color figure can be viewed at wileyonlinelibrary.com]

selected pressures in Figure 2. As seen from the figure, the pair correlation functions present a clear short-range peak and the lack of long-range correlations during the entire pressurization process, suggesting that TiO_2 remains amorphous at the highest pressure achieved at the present work and undergoes polyamorphic phase transformation(s). Note the appearance of a visible peak at around 2.88 Å and 3.16 Å, which indicate the occurrence of the medium-range order due to the crystalline-like topologies (probably eight-fold-coordinated units as they are the most dominated ones at 75 GPa, see below).

Coordination number (CN) is one of the useful parameters to detect pressure-induced structural phase transformations in materials. Therefore, we next probe the modification of the partial average CNs under pressure and provide them in Figure 3. The mean CNs are predicted from the first minimum of the correlation functions. At ambient pressure, the average CN of Ti and O atoms is 5.3 and 2.38, respectively, comparable with the earlier investigations.[39,40] The Ti and O CNs remain nearly constant between 0 GPa and 20 GPa. After 20 GPa they begin to increase progressively. It becomes 6.72 for Ti atom and 3.36 for O atom at 55 GPa. At 60 GPa, the mean CN of Ti and O atoms sharply increases to 7.75 and 3.87, correspondingly. The increase in the CNs at this pressure is ~16%.

To have more information about the topology of the amorphous state at high pressures, we carefully explore the clustering of Ti and O atoms in the model and plot their coordination distribution at each applied pressure in Figure 4. The amorphous network does have an

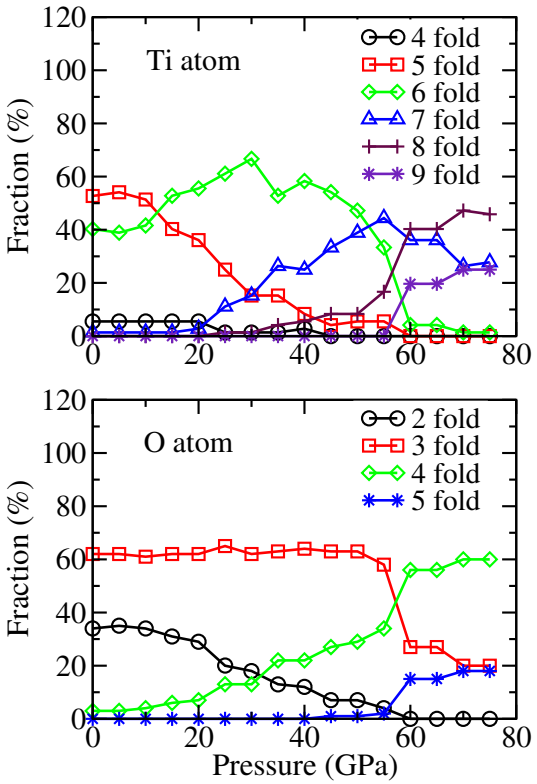

FIGURE 4 The coordination distribution of Ti and O atoms at each applied pressure [Color figure can be viewed at wileyonlinelibrary.com]

inhomogeneous coordination distribution unlike the crystalline phases. At zero pressure, the fivefold- and sixfold-coordinated arrangements are the most prevalent ones,

which are octahedrons and pyramidal-shaped incomplete octahedrons, respectively. The number of the fivefold-coordinated configurations substantially decreases beyond 20 GPa and becomes insignificantly small at 45 GPa. On the other hand, the amount of the sixfold coordination under pressure increases initially, reaches a maximum value at 30 GPa, and then starts to decrease continuously up to 60 GPa at which point it drops a negligibly small value. The sevenfold coordination arises at 25 GPa and has a maximum value at 55 GPa. With increasing the applied pressure to 60 GPa it discontinuously declines to a small value. The eightfold coordination first develops at 25 GPa and its fraction increases considerably between 50 and 60 GPa. The ninefold-coordinated topologies appear at 60 GPa and more develop at higher pressures. The formation or modification of higher coordinated configurations (sevenfold, eightfold, and ninefold) in a-TiO_2, similar to the high-pressure behavior of the crystalline TiO_2 (Refs 41-47), can be inferred as a possible structural phase transformation between 25 GPa and 55 GPa and at 60 GPa.

Upon decompression from 75 GPa, the average CN of Ti and O atoms slowly decreases and reaches 6.58 and 3.29 at zero pressure, respectively (Figure 3). When the applied pressure is released from 55 GPa, the resulting average CNs at zero pressure are 5.94 and 2.97 (see Figure 3). For both cases, one can see that the original CNs and density are not recovered. However, the CNs (6.58 and 3.29) obtained at zero pressure during the pressure release from 75 GPa are comparable with 6.5 (6.72) and 3.25 (3.36) achieved at 50 (55) GPa during the compression process, although the amorphous networks at these pressures have significantly different densities (see Figure 1). In addition, a careful analyze suggests that the coordination distribution of these amorphous models are fairly close to each other. Therefore, we conclude that the VHDA-HDA phase transformation is reversible while the HDA-to-LDA phase change is irreversible.

The coordination distribution of the original and decompressed amorphous materials is shown in Figure 5 to reveal their fundamental structural distinctions. Upon pressure release, we observe the persistence of a nonnegligible amount of the sevenfold and eightfold clusters (these are high-pressure configurations) and the privilege of sixfold-coordinated arrangements in the system. Note that the fivefold-coordinated clusters are the most preferred one in the original amorphous network. Therefore, the recovered amorphous materials notably differ from each other and the original amorphous configuration. These findings indicate the existence of different HDA phases of TiO_2 with diverse densities and CNs, according with the experimental observations in the nanostructured TiO_2 materials.[29]

To provide additional information regarding the microstructure of a-TiO_2 under pressure, we study the

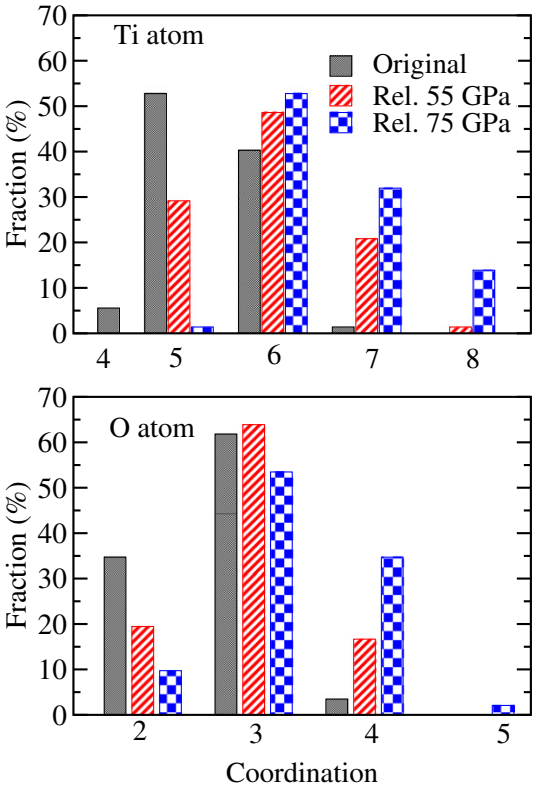

FIGURE 5 The coordination distribution of the initial and decompressed amorphous networks [Color figure can be viewed at wileyonlinelibrary.com]

Ti-O-Ti and O-Ti-O angle distributions and present them in Figure 6. At ambient pressure, the Ti-O-Ti angle distribution exhibits peaks at ~100° and 128° and a shoulder at ~151°, whereas the O-Ti-O distribution shows peaks at ~76°, 90°, and 98°. For the anatase phase, the Ti-O-Ti peaks are placed at 101.9° and 156.2° and for the rutile phase, the peaks are located at 98.8° and 130.6°. The anatase crystal produces the O-Ti-O angles at 78.1°, 92.4°, 101.9°, and 156.2° and whereas the rutile state leads to the O-Ti-O angles at 90°, 81.2°, 98.2°, and 180°. So one can easily see that our amorphous model is structurally closer to the rutile crystal than the anatase crystal. As the applied pressure is increased, we observe drastic changes in the both angle distribution functions. In the Ti-O-Ti distribution, the peak positioned at ~128° is gradually suppressed and almost disappeared at 30-35 GPa, while the peak around 100° is slowly broadened. In the O-Ti-O angle distribution, the main peaks at ~76°, 90°, and 98° merge and produce a sharp peak at ~77°. In addition, a broad new peak around 145° develops gradually after 45 GPa.

Note that due to the presence of differently coordinated motifs in the amorphous network, from the bond-angle distribution functions, it is indeed hard to uncover a relation between the local structure of the compressed a-TiO_2 state

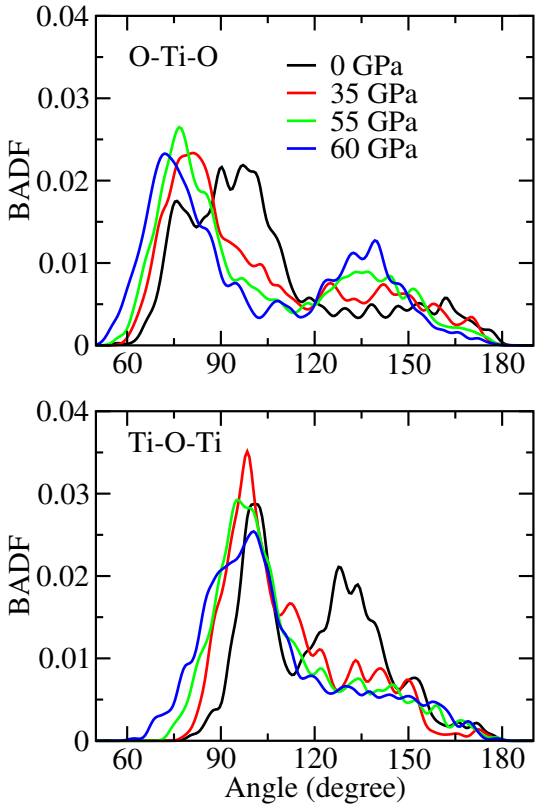

FIGURE 6 The Ti-O-Ti and O-Ti-O bond-angle distribution functions at selected pressures [Color figure can be viewed at wileyonlinelibrary.com]

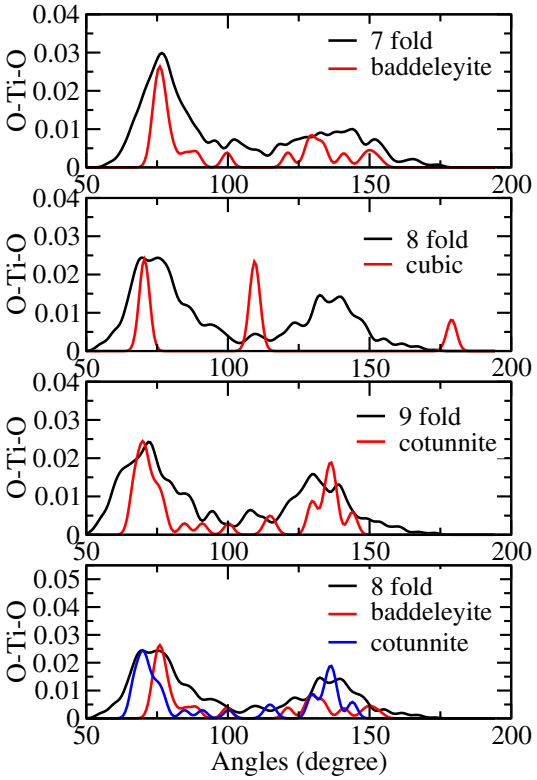

FIGURE 7 The O-Ti-O bond-angle distribution of the sevenfold configurations at 55 GPa, eightfold and ninefold arrangements at 60 GPa along with that of the high-pressure crystalline TiO_2 phases [Color figure can be viewed at wileyonlinelibrary.com]

and that of the high-pressure crystalline TiO_2 phases because each type of clusters formed under pressure might produce particular angles that sometime overlap and lead to wide-angle distributions. The relation between the crystalline and amorphous states of TiO_2 can be revealed by solely focusing on the particular clusters formed in *a*-TiO_2 at high pressures. The sevenfold-, eightfold-, and ninefold-coordinated configurations are extracted from the amorphous model at 55 and 60 GPa and their O-Ti-O distribution along with that of the high-pressure crystalline TiO_2 phases are computed and plotted in Figure 7. As understood from the figure, the sevenfold- and ninefold-coordinated structures in the amorphous network have a microstructure, rather similar to that of the high-pressure baddeleyite and cotunnite phases of TiO_2. On the other hand, we find no resemblance between the eightfold-coordinated units and the local structure of the cubic TiO_2 phase.[41] However, the bond-angle distribution of the eightfold-coordinated structures appears to be close to that of the baddeleyite and cotunnite phases. The cluster analysis using the Voronoi polyhedra technique proposes that there is only one type of eightfold-coordinated polyhedron with an index of <0 4 4 0> formed in *a*-TiO_2, which seems to be relatively close to the polyhedron of the badaliyette crystal (<1 3 3 0>) and contunitte phase (<0 3 6 0>) as shown in Figure 8. So on the basis of our findings from the bond-angle distribution and cluster analyses, we call this eightfold-coordinated unit as an *intermediate*

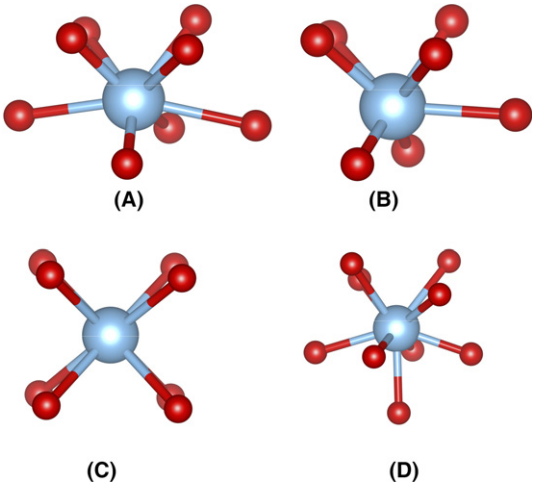

FIGURE 8 (A) Eightfold-coordinated polyhedron formed in *a*-TiO_2 under pressure. (B) Sevenfold-coordinated polyhedron of the baddeleyite phase. (C) Eightfold-coordinated polyhedron of the cubic phase. (D) Ninefold-coordinated polyhedron of the cotunnite crystal. Large and small spheres are Ti and O atoms, respectively [Color figure can be viewed at wileyonlinelibrary.com]

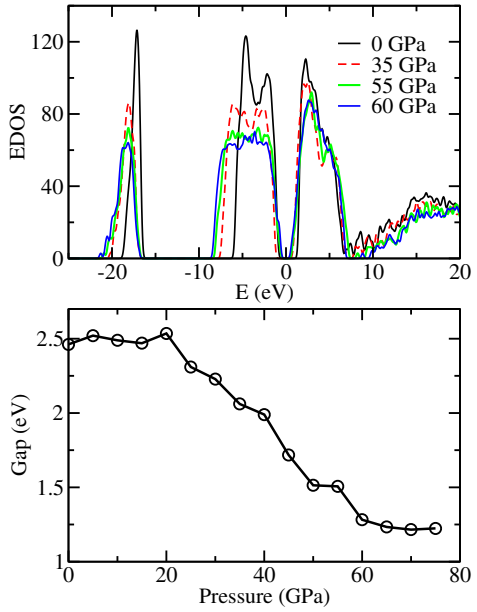

FIGURE 9 The electron density of states. The Fermi level is at 0 eV. The variation in band gap energy with the application of pressure [Color figure can be viewed at wileyonlinelibrary.com]

configuration between the baddeleyite and cotunnite structures.

We lastly consider the impact of compression on the electronic properties of a-TiO_2. The computed electronic density of states at specific pressures and the change in the band gap as a function of pressure are given in Figure 9. At zero pressure, the band gap energy is about 2.5 eV, slightly greater than the previous theoretical result of about 2.0 eV.[39] The band gap energy remains almost constant between 0 GPa and 20 GPa. After 20 GPa, it has a trend to decrease and reaches nearly a constant value above 60 GPa. So based on this observation we can conclude that the coordination modification considerably affects the electronic structure of a-TiO_2, but its metallization does not occur up to 75 GPa. Nevertheless, from a linear fit of the band gap above 20 GPa, the metallization of a-TiO_2 is crudely projected to occur at a theoretical pressure of 115 GPa. This estimation includes the self-interaction error (under estimation of band gap energy) in DFT-GGA calculations and hence it is a quite rough projection. Therefore, we also try to guess the metallization pressure of a-TiO_2 from the variation in the mean CN of Ti atom as the metallization of the crystalline TiO_2 appears when the CN of Ti is 10 (Refs 42,43). The mean CN of Ti from a linear fit beyond 60 GPa is anticipated to be 10 at around 180 GPa, close to the value predicted from the variation in the band gap energy under pressure. Consequently the metallization of a-TiO_2 is expected to occur roughly at 180 GPa if and only if the pressure-induced structural modifications continue in this manner. We should point out here that this prediction is much less than the metallization pressure, 647-60 GPa[42,43], of the crystalline TiO_2.

4 | DISCUSSION

On the basis of the variation in coordination, volume, and even band gap energy under pressure, we propose two successive polyamorphic phase transformations in a-TiO_2. The first one corresponds to a continuous-phase change from a LDA phase to a HDA phase between 25 GPa and 55 GPa. The second one is a first-order phase transformation from the HDA phase to a VHDA phase at 60 GPa.

One might argue that about 5% volume collapse at 60 GPa is rather small to be considered as a first-order phase transformation and it might be a finite-size artifact. Indeed, it is probable that our conclusion on the thermodynamic character of the second-phase transformation can be associated with the small size of the model, but this does not invalidate the existence of a VHDA phase in a-TiO_2. Nonetheless, we would like to point out here that the change in the CNs at this pressure is about 16% and in the crystalline forms of TiO_2, the phase change from the sevenfold-coordinated structure to the eightfold-coordinated structure requires ~15% coordination increase. In addition, the transition from the sevenfold-coordinated orthorhombic crystal (space group: *Pbca*) to the ninefold-coordinated cotunnite crystal involves around 8% volume decline.[45] Consequently, it is quite reasonable to consider the phase change at 60 GPa as a first-order phase transformation.

Both HDA and VHDA phases involve differently coordinated structures. Such a finding is predictable and was reported in other materials showing an amorphous-to-amorphous phase transformation as well.[3,8] Noted that at ambient condition, the model contains structural defects (angular distortions, coordination defects, and bond-length disorder), which can lead to additional freedom for some atoms in the model to attain higher-coordinated clusters under pressure. So the structural defects are mainly responsible for the formation of the differently coordinated configurations in a-TiO_2 at high pressures.

The HDA phase obtained in nanoscale TiO_2 systems with increasing pressure is suggested to resemble locally to the badaliyete crystal.[25,28,30] In a contrast to this suggestion, we see that the HDA phase of a-TiO_2 consists of the sixfold-coordinated rutile- or columbite-type crystals, the sevenfold-coordinated badaliyete-type phase (dominated at 55 GPa), and the eightfold-coordinated *intermediate* arrangement. The VHDA phase, on the other hand, involves the badaliyete-type crystal, the eightfold-coordinated *intermediate* cluster, and the cotunnite-type phase.

On decompression from two different pressures, the original density and configurations are not recovered. This

means that the LDA-HDA phase transformation in bulk a-TiO_2 is irreversible in a contrast to the prediction in the nanostructured TiO_2 materials.[29] However, as discussed above, upon decompression from 75 GPa, an amorphous phase, parallel to the HDA state observed during the compression at 50-55 GPa, is recovered, suggesting that the VHDA-HDA phase change is reversible.

The experimental high-pressure investigation on TiO_2 nanoparticles reveals that depending on the initial structure, it is possible to have multiple HDA phases (labeled as HDA1 and HDA2) and there is a phase transformation from the HDA2 phase to the HDA1 phase.[29] The structure of these HDA phases was not identified in that study because of the weak Raman spectra peaks. Indeed, we also propose that there exist structurally different HDA phases for bulk TiO_2 as we obtain dissimilar amorphous states on both compression and decompression from different pressures. However, we believe that neither HDA1 phase nor HDA2 phase corresponds to the VHDA configuration predicted in this study because the HDA2 phase was proposed to be an intermediate phase between the LDA and HDA structures.[29]

The structural analyses reveal some similarities and distinctions concerning the polyamorphic phase transition in the nanoscale TiO_2 materials and bulk TiO_2 systems. It is indeed rather unreasonable to expect to have precisely the same findings for two different forms of TiO_2 because for nanostructured TiO_2, many factors such as its size, surface energy, shape etc. yield different physical phenomenon including pressure-induced phase transformations, relative to bulk TiO_2.

It might be interesting to explore a-TiO_2 under different stress conditions such as uniaxial, biaxial, and nonhydrostatic stresses because such studies could be helpful to better understand its solid-solid phase transformations. Furthermore, these types of investigations might shed some lights on the atomic structure of nanoscale a-TiO_2 materials as they experience important *intrinsic* comprehensive stresses that depend on their geometries (cross-sectional shapes) and sizes.

The crystalline TiO_2 has a rich phase diagram and attains sixfold-, sevenfold-, eightfold- (still remains controversy about the structure of this phase[44]), ninefold-, and tenfold-coordinated structures at high-temperature and pressure conditions.[41–47] Consequently, the average CN of the amorphous states of TiO_2 obtained in the present simulations practically corresponds to that of the crystalline polymorphs. At higher pressures, a transformation into more densely packed amorphous structures having ninefold and tenfold coordination is likely to occur in TiO_2 unless the crystallization is favorable.

The eightfold-coordinated configuration formed in TiO_2 under pressure appears to be different from the local structure of the cubic TiO_2 phase. The observation of such a different configuration might suggest that (1) the disorder nature of a-TiO_2 may favor the development of such a local arrangement such that it cannot occur in any crystalline TiO_2 states, (2) as observed in a-AlN[36], it can be a main building unit of an intermediate crystalline phase that connects the sevenfold-coordinated baddeleyite phase to the ninefold-coordinated cotunnite phase during the phase transformation, and (3) a new stable crystalline structure consisting of the intermediate eightfold-coordinated motif, different than the cubic TiO_2 phase, might exist and can form in TiO_2 under some specific temperature and pressure conditions. Additional theoretical and experimental studies on the baddeleyite crystal and a-TiO_2 at high-temperature and pressure environments are needed to clarify this issue.

We finally note here that the proposed LDA-HDA and HDA-VHDA structural phase transformations are expected to start/occur at a lower pressure in experiments because the critical/starting pressures predicted in dynamical simulations are usually overvalued due to some limitations in simulations such as nonexistence of surface effects, rapid pressurizing, etc. Furthermore, the overestimated pressures in simulations lead to the transition parameters such as transition's volumes and the amount of the volume collapse etc. that cannot be compared with experimental values.

5 | CONCLUSIONS

We have explored the high-pressure behavior of a-TiO_2 and propose two successive amorphous-to-amorphous phase transformations. The first phase change proceeds continuously from a LDA state to a HDA state, whereas the second one occurs in a first-order nature from the HDA phase to a VHDA phase. The LDA-to-HDA phase transformation is irreversible because the original amorphous state and density are not recovered upon pressure release. On the other hand, the VHDA-to-HDA phase change is reversible. We propose that there exist multiple HDA phases with diverse densities and coordination environments in TiO_2. The HDA and VHDA phases consist of distinct coordination environments. The sevenfold- and ninefold-coordinated arrangements formed in a-TiO_2 under pressure resemble the local structure of the baddeleyite and cotunnite polymorphs of TiO_2, respectively, whereas the eightfold-coordinated configuration is different than the local arrangement of the cubic TiO_2 phase. The electronic structure calculations suggest that both HDA and VHDA phases exhibit a semiconducting behavior.

ACKNOWLEDGMENTS

This work was partially supported by the Abdullah Gül University Support Foundation. The calculations were run

on TÜBİTAK ULAKBİM, High Performance and Grid Computing Center (TRUBA resources).

REFERENCES

1. Poole PH, Grande T, Sciortino F, et al. Amorphous polymorphism. *Comput Mater Sci*. 1995;4:322-373.
2. Mishima O, Calvert LD, Whalley E. An apparently first-order transition between two amorphous phases of ice induced by pressure. *Nature*. 1985;314:76-78.
3. Durandurdu M, Drabold DA. Ab initio simulation of first-order amorphous-to-amorphous phase transition of silicon. *Phys Rev B*. 2001;64:014101-014107.
4. Durandurdu M. Ab initio simulation of polyamorphic phase transition in hydrogenated silicon. *Phys. Rev B*. 2006;73:035209-0352015.
5. Deb SK, Wilding M, Somayazulu M, et al. Pressure-induced amorphization and an amorphous–amorphous transition in densified porous silicon. *Nature*. 2001;414:528-530.
6. McMillan PF, Wilson M, Daisenberger D, et al. A density-driven phase transition between semiconducting and metallic polyamorphs of silicon. *Nat Mater*. 2005;4:680-684.
7. Principi E, Decremps F, Di Cicco A, et al. Pressure induced phase transitions in amorphous Ge. *Phys Scr*. 2005;T115:381-383.
8. Durandurdu M, Drabold DA. First-order pressure-induced polyamorphism in germanium. *Phys Rev B*. 2002;66:041201-041204.
9. Li N, Sakidja R, Aryal S, et al. Densification of a continuous random network model of amorphous SiO_2 glass. *Phys Chem Chem Phys*. 2014;16:1500-1514.
10. Guerette M, Ackerson MR, Thomas J, et al. Structure and properties of silica glass densified in cold compression and hot compression. *Sci Rep*. 2015;5; Article number 15343.
11. Zeidler A, Wezka K, Rowlands RF, et al. High-pressure transformation of SiO_2 glass from a tetrahedral to an octahedral network: A joint approach using neutron diffraction and molecular dynamics. *Phys Rev Lett*. 2014;113:135501-135505.
12. Tsiok OB, Brazhkin VV, Lyapin AG, et al. Logarithmic kinetics of the amorphous-amorphous transformations in SiO_2 and GeO_2 glasses under high pressure. *Phys Rev Lett*. 1998;80:999-1002.
13. Salmon PS, Drewitt JW, Whittaker DA, et al. Density-driven structural transformations in network forming glasses: a high-pressure neutron diffraction study of GeO_2 glass up to 17.5 GPa. *J Phys: Condens Matter*. 2012;24:415102-415117.
14. Brazhkin VV, Bychkov E, Tsiok OB. Direct volumetric study of high-pressure driven polyamorphism and relaxation in the glassy germanium chalcogenides. *J Phys Chem B*. 2016;120:358-363.
15. Durandurdu M, Drabold DA. Simulation of pressure-induced polyamorphism in a chalcogenide glass $GeSe_2$. *Phys Rev B*. 2002;65:104208-104215.
16. Properzi L, Di Cicco A, Nataf L, et al. Short-range order of compressed amorphous $GeSe_2$. *Sci Rep*. 2015;5; Article number 10188.
17. Properzi L, Santoro M, Minicucci M, et al. Structural evolution mechanisms of amorphous and liquid As_2Se_3 at high pressures. *Phys Rev B*. 2016;93:214205-214212.
18. Mishima O. Relationship between melting and amorphization of ice. *Nature*. 1996;384:546-549.
19. Loerting T, Salzmann C, Kohl I, et al. A second distinct structural "state" of high-density amorphous ice at 77 K and 1 bar. *Phys Chem Chem Phys*. 2001;3:5355-5357.
20. Loerting T, Brazhkin VV, Morishita T. Multiple amorphous-amorphous transitions. *Adv Chem Phys*. 2009;143:29-82.
21. Yavari AR. Metallic glasses: The changing faces of disorder. *Nat Mater*. 2007;6:181-182.
22. Sheng HW, Liu HZ, Cheng YQ, et al. Polyamorphism in a metallic glass. *Nat Ater*. 2007;6:192-197.
23. Lou HB, Fang YK, Zeng QS, et al. Pressure-induced amorphous-to-amorphous configuration change in Ca-Al metallic glasses. *Sci Rep*. 2012;2; Article Number 376.
24. Zeng QS, Fang YZ, Lou HB, et al. Low-density to high-density transition in $Ce_{75}Al_{23}Si_2$ metallic glass. *J Phys: Condens Matter*. 2010;22:375404-375407.
25. Li Q, Liu B, Wang L, et al. Pressure-induced amorphization and polyamorphism in one-dimensional single-crystal TiO_2 nanomaterials. *J Phys Chem Lett*. 2009;1:309-314.
26. Swamy V, Kuznetsov A, Dubrovinsky LS, et al. Size-dependent pressure-induced amorphization in nanoscale TiO_2. *Phys Rev Lett*. 2006;96:135702-135704.
27. Swamy V, Muddle BC. Pressure-induced polyamorphic transition in nanoscale TiO2. *J Aust Ceram Soc*. 2008;44:1-5.
28. Swamy V, Kuznetsov AY, Dubrovinsky LS, et al. Unusual compression behavior of anatase TiO_2 nanocrystals. *Phys Rev Lett*. 2009;103:075505-075508.
29. Machon D, Daniel M, Pischedda V, et al. Pressure-induced polyamorphism in TiO_2 nanoparticles. *Phys Rev B*. 2010;82:140102-140104.
30. Flank AM, Lagarde P, Itié JP, et al. Pressure-induced amorphization and a possible polyamorphism transition in nanosized TiO_2: An x-ray absorption spectroscopy study. *Phys Rev B*. 2008;77:224112-224120.
31. Pischedda V, Hearne GR, Dawe AM, et al. Ultrastability and enhanced stiffness of $\sim$6 nm TiO_2 nanoanatase and eventual pressure-induced disorder on the nanometer scale. *Phys Rev Lett*. 2006;96:035509-0355012.
32. Ordejón P, Artacho E, Soler JM. Self-consistent order-N density-functional calculations for very large systems. *Phys Rev B*. 1996;53:R10441-R10444.
33. Parrinello M, Rahman A. Polymorphic transitions in single crystals: A new molecular dynamics method. *J Appl Phys*. 1981;52:7182-7190.
34. Perdew JP, Burke K, Ernzerhof M. Generalized gradient approximation made simple. *Phys Rev Lett*. 1996;77:3865-3868.
35. Troullier N, Martins JL. Efficient pseudopotentials for plane-wave calculations. *Phys Rev B*. 1991;43:993-2006.
36. Durandurdu M. Polyamorphism in aluminum nitride: A first principles molecular dynamics study. *J Am Ceram Soc*. 2016;99:1594-1600.
37. Le Roux S, Petkov V. ISAACS–interactive structure analysis of amorphous and crystalline systems. *J Appl Crystallogr*. 2010;43:181-185.
38. Medvedev NN. The algorithm for three-dimensional voronoi polyhedral. *J Comput Phys*. 1986;67:223-229.
39. Prasai B, Cai B, Underwood MK, et al. Properties of amorphous and crystalline titanium dioxide from first principles. *J Mater Sci*. 2012;47:7515-7521.
40. Petkov V, Holzhüter G, Tröge U, et al. Atomic-scale structure of amorphous TiO_2 by electron, X-ray diffraction and reverse Monte Carlo simulations. *J Non-Cryst Solids*. 1998;231:17-30.

41. Mattesini M, De Almeida JS, Dubrovinsky L, et al. High-pressure and high-temperature synthesis of the cubic TiO_2 polymorph. *Phys Rev B*. 2004;70:212101-212104.
42. Zhong X, Wang J, Zhang S, et al. Ten-fold coordinated polymorph and metallization of TiO_2 under high pressure. *RSC Adv*. 2015;5:54253-54257.
43. Lyle MJ, Pickard CJ, Needs RJ. Prediction of 10-fold coordinated TiO_2 and SiO_2 structures at multimegabar pressures. *PNAS*. 2015;112:6898-6901.
44. Liang Y, Zhang B, Zhao J. Mechanical properties and structural identifications of cubic TiO_2. *Phys Rev B*. 2008;77:094126-094131.
45. Al-Khatatbeh Y, Lee KK, Kiefer B. High-pressure behavior of TiO_2 as determined by experiment and theory. *Phys Rev B*. 2009;79:34114-34122.
46. Dubrovinskaia NA, Dubrovinsky LS, Ahuja R, et al. Experimental and theoretical identification of a new high-pressure TiO_2 polymorph. *Phys Rev Lett*. 2001;87:275501-275504.
47. Muscat J, Swamy V, Harrison NM. First-principles calculations of the phase stability of TiO_2. *Phys Rev B*. 2002;65:224112-224126.

How to cite this article: Durandurdu M. Two successive amorphous-to-amorphous phase transformations in TiO_2. *J Am Ceram Soc*. 2017;100:3903–3911. https://doi.org/10.1111/jace.14947